

Synthesis, characterization and catalytic activity for NO–CO reaction of Pd–(La, Sr)₂MnO₄ system

R. Karita^a, H. Kusaba^b, K. Sasaki^b, Y. Teraoka^{b,*}

^a Department of Molecular and Material Sciences, Interdisciplinary Graduate School of Engineering Sciences, Kyushu University, Kasuga, Fukuoka 816-8580, Japan

^b Department of Energy and Material Sciences, Faculty of Engineering Sciences, Kyushu University, Kasuga, Fukuoka 816-8580, Japan

Available online 11 September 2006

Abstract

La_xSr_{2-x}MnO₄ (0 ≤ x ≤ 0.8) oxides were synthesized and single-phase K₂NiF₄-type oxides were obtained in the range of 0.1 ≤ x < 0.5. The catalytic activity of La_xSr_{2-x}MnO₄ for NO–CO reaction increased with increasing x in the range of solubility limit of La. La_{0.5}Sr_{1.5}MnO₄ showed the highest activity among La_xSr_{2-x}MnO₄ prepared in this study, but its activity was inferior to perovskite-type La_{0.5}Sr_{0.5}MnO₃. Among the Pd-loaded catalysts, however, Pd/La_{0.8}Sr_{1.2}MnO₄ showed the higher activity and the selectivity to N₂ than Pd/La_{0.5}Sr_{0.5}MnO₃ and Pd/γ-Al₂O₃. The excellent catalytic performance of Pd/La_{0.2}Sr_{1.2}MnO₄ could be ascribable to the formation of SrPd₃O₄ which was detected by XRD in the catalyst but not in the other two catalysts.

© 2006 Elsevier B.V. All rights reserved.

Keywords: Pd; SrPd₃O₄; NO–CO reaction; La_xSr_{2-x}MnO₄

1. Introduction

Perovskite-type oxides have been attracting a great deal of attention in environmental-related catalytic fields, because they show high catalytic activity for NO_x removal and the oxidation of CO and VOC [1]. Recently, Pd-containing perovskites such as La(Fe, Co, Pd)O₃ are reported to have self-regeneration property. Pd in perovskite is reduced under the rich condition, and the reduced Pd metal is oxidized and re-dissolved in the perovskite lattice under the lean condition [2,3]. This self-regeneration function is said to be quite effective to suppress the growth of Pd metal particles and they are successfully put into practical use in three-way catalytic converter.

As a new support or matrix for active Pd species, we have been investigating K₂NiF₄-type oxides. In K₂NiF₄-type oxide (A₂BO₄), A is a larger metal cation such as rare earth and alkaline earth metal ions and B is a smaller one like transition metal ions. Although the structure of the K₂NiF₄-type oxide is related to the perovskite oxide (ABO₃) and A- and B-site cations are usually common to both oxide systems, reports on

the catalytic properties of K₂NiF₄-type oxides are limited as compared with those of perovskite-type oxides. When a trivalent rare earth cation (Ln³⁺) are used as the A-site cation, the B-site cation should basically take a trivalent state in perovskite (Ln³⁺B³⁺O₃) and a divalent one in K₂NiF₄-type (Ln₂³⁺B²⁺O₄). This is a reason why transition metal cations at B site of the K₂NiF₄-type oxides reported as catalytic materials were limited to Co, Cu and Ni [4–14]. Since Mn-containing perovskites are well known to exhibit high catalytic activity, it is worth studying the catalytic property of Mn-containing K₂NiF₄-type oxides. It is reasonable that the divalent A-site cation should be used as the main A-site cation (A²⁺₂B⁴⁺O₄) instead of the trivalent one (A₂³⁺B²⁺O₄), because Mn takes a tetravalent state easier than a divalent one under the ordinary preparation condition like calcination in air.

In this paper, Mn-containing K₂NiF₄-type oxides, La_xSr_{2-x}MnO_{4+δ} (0 ≤ x ≤ 0.8), and Pd/La_xSr_{2-x}MnO₄ (x = 0.2) were synthesized, and their crystal structures and catalytic performance toward the NO–CO reaction have been investigated.

2. Experimental

La_xSr_{2-x}MnO₄ (0 ≤ x ≤ 0.8) were prepared by the air-calcination (800 °C) of the precursor obtained by an evaporation-

* Corresponding author. Tel.: +81 92 583 7526; fax: +81 92 583 8853.

E-mail address: teraoka@mm.kyushu-u.ac.jp (Y. Teraoka).

to-dryness method using nitrates of La, Sr and Mn(II) as starting materials. $\text{La}_{0.2}\text{Sr}_{1.8}\text{MnO}_4$ thus prepared was suspended in aqueous $\text{Pd}(\text{NO}_3)_2$ (pH 6–8) followed by evaporation-to-dryness and air-calcination at 800 °C. The loading of Pd was set at 5 wt.%. Crystal phases in the products were identified by powder X-ray diffraction (XRD) using Cu K α radiation (Rigaku RINT2200). Specific surface areas of catalysts were measured by N_2 adsorption at liquid N_2 temperature (BET method) using NOVA2200 (Yuasa Ionics Inc.). Contents of Mn(III) and Mn(IV) in $\text{La}_x\text{Sr}_{2-x}\text{MnO}_4$ ($0 \leq x \leq 0.6$) were measured by iodometric analysis [15]. Since they showed nonstoichiometry as described below, the oxides should be expressed as $\text{La}_x\text{Sr}_{2-x}\text{MnO}_{4+\delta}$. In this paper, however, we used $\text{La}_x\text{Sr}_{2-x}\text{MnO}_4$ for simplicity.

Temperature programmed desorption (TPD) of oxygen was measured by BELCAT (BEL JAPAN INC). The heating rate was 10 °C min⁻¹, and the desorbed oxygen was monitored by a thermal conductivity-type detector. The pretreatment was as follows. The catalyst sample was heated up to and kept for 10 min at 800 °C under a flow of helium. After replacing the He flow by a flow of synthetic air and keeping for 30 min at the same temperature, the sample was cooled down to room temperature.

Catalytic activity for NO–CO reaction was measured with a fixed-bed flow reactor of quartz tubing. A gaseous mixture of 0.542% NO, 0.516% CO and He (balance) was fed to the catalyst bed (0.3 g) at a space velocity (SV) of 37,500 h⁻¹. Inlet and outlet gases were analyzed by an on-line gas chromatography (Shimadzu, GC-14B). The steady-state results were obtained after passing 1 h or more at each reaction temperature. X-ray photoelectron spectra (XPS) were recorded on an ESCA3400 (Shimadzu) with an Mg K α radiation. Binding energy (BE) was calibrated with reference to C1s_{1/2} level of contaminant carbon at 284.6 eV. The dissolution of oxides during suspending in water at room temperature was measured by analyzing the concentration of metal cations in water by X-ray fluorescence spectrometer (Rigaku ZSXmini; He atmosphere; Pd radiation source).

3. Results and discussion

3.1. Characterization of materials

According to the discussion in Section 1, Sr_2MnO_4 was selected as the base materials, because the Mn ion takes tetravalence if the stoichiometric compound is formed. Fig. 1 shows XRD patterns of the $\text{La}_x\text{Sr}_{2-x}\text{MnO}_4$ ($0 \leq x \leq 0.8$) prepared in this study. The XRD pattern of the oxide with $x = 0$ agreed with that of the so-called $\alpha\text{-Sr}_2\text{MnO}_4$ [16], the structure of which is different from the K_2NiF_4 -type structure. It was reported that $\alpha\text{-Sr}_2\text{MnO}_4$ transformed into the K_2NiF_4 -type structure above 1600 °C [16]. When 5% of Sr was substituted with La ($x = 0.1$), XRD pattern was completely different from that of $\alpha\text{-Sr}_2\text{MnO}_4$ ($x = 0$), and all the diffraction peaks could be indexed on the basis of tetragonal K_2NiF_4 -type structure. Any diffraction peaks from impurity phases were not observed for $x = 0.1$ – 0.4 , suggesting the formation of single-phase K_2NiF_4 -type oxides up to $x = 0.4$. At higher x values, on the other hand,

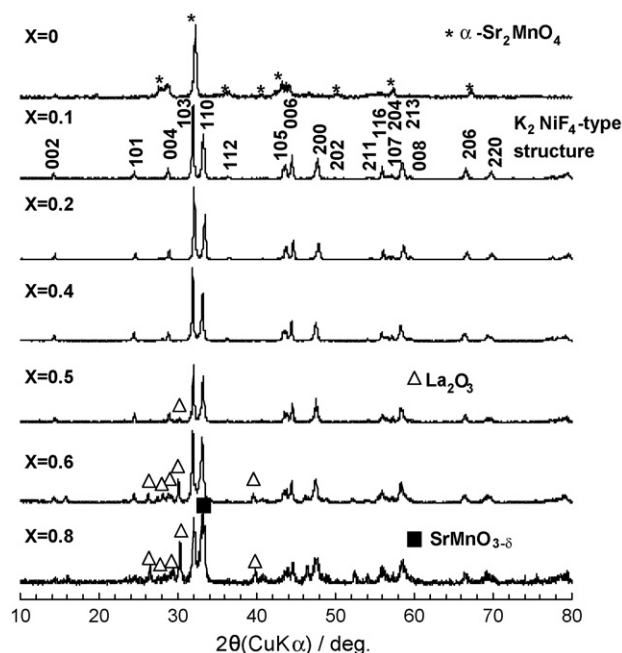


Fig. 1. XRD patterns of $\text{La}_x\text{Sr}_{2-x}\text{MnO}_4$ ($0 \leq x \leq 0.8$).

the formation of by-products was observed. La_2O_3 was formed in oxides of $x = 0.5$, 0.6 and 0.8 , and the amount of La_2O_3 increased with increasing x . Judging from the relative intensities of two strongest peaks around 33°, the formation of $\text{SrMnO}_{3-\delta}$ was sure for the oxide of $x = 0.8$. It can be concluded that the solubility limit of La^{3+} in $\text{La}_x\text{Sr}_{2-x}\text{MnO}_4$ is just below 0.5 under the present preparation condition.

Table 1 summarizes composition calculated from the iodometry results and lattice parameters of $\text{La}_x\text{Sr}_{2-x}\text{MnO}_4$ ($0.1 \leq x \leq 0.5$), which were obtained as pure ($x \leq 0.4$) and nearly pure ($x = 0.5$) K_2NiF_4 -type oxides. With increasing the La content, the nonstoichiometry changed from the oxygen-deficient ($x = 0.1$) to oxygen-excess ($x = 0.4$ and 0.5) compositions by way of the almost stoichiometric composition at $x = 0.2$. The change in oxygen nonstoichiometry from the excess to deficient compositions with increasing Sr content has been often observed in K_2NiF_4 -type oxides containing Co and Ni at B site [5–8,11,12]. The A-site composition, at which the excess-to-deficient transition of oxygen composition occurs, depends on the B-site cations. If the oxide is expressed as $\text{La}_{2-y}\text{Sr}_y\text{BO}_4$, the transition takes place around $y = 0.5$ for Ni [6,8,11,12], around $y = 1.0$ – 1.2 for Co [5,7] and around $y = 1.8$

Table 1
Unit cell parameters and composition of $\text{La}_x\text{Sr}_{2-x}\text{MnO}_4$ ($0.1 \leq x \leq 0.5$)

x	Lattice parameter			Composition of $\text{La}_x\text{Sr}_{2-x}\text{Mn}_{p^{3+}}\text{Mn}_{q^{4+}}\text{O}_z$			Specific surface area (m ² /g)
	a (Å)	c (Å)	V (Å ³)	p	q	z	
0.1	3.81	12.41	180.1	0.27	0.73	3.92	1.4
0.2	3.80	12.29	177.4	0.22	0.78	3.99	2.2
0.4	3.81	12.41	180.1	0.24	0.76	4.08	2.8
0.5	3.82	12.44	181.5	0.30	0.70	4.10	4.3

as found in this study. The difference in the transition composition can be reasonably understood on the basis of oxidation states which the B site cation takes stably in the oxide; $2 + 1/3 +$ for Ni, $2 + 1/3 + 1/4 +$ for Co and $3 + 1/4 +$ for Mn.

All these oxides crystallized in the tetragonal K_2NiF_4 -type structure, and the unit cell volume (V) changed with x as $0.2 < 0.1 = 0.4 < 0.5$. This order can be basically explained from the relative composition of larger Mn^{3+} and smaller Mn^{4+} ; the proportion of Mn^{3+} was the highest in the oxide ($x = 0.5$) having the largest V and the lowest in the oxide ($x = 0.2$) with the smallest V .

It has turned out that the formation of single-phase K_2NiF_4 -type oxide in the $La_xSr_{2-x}MnO_4$ system is realized by the substitution of La for Sr in the range of $0.1 \leq x < 0.5$ after air-calcination at 800 °C. The lowering of the formation temperature, as compared with 1600 °C for Sr_2MnO_4 [16], made it possible to apply these oxides for catalytic materials, although the specific surface areas were not so large (Table 1).

XRD patterns of three Pd-loaded catalysts, Pd/ $La_{0.2}Sr_{1.8}MnO_4$, Pd/ $La_{0.5}Sr_{0.5}MnO_3$ and Pd/ $\gamma-Al_2O_3$, are shown in Fig. 2. Loaded Pd was present as PdO on $\gamma-Al_2O_3$ and perovskite-type $La_{0.5}Sr_{0.5}MnO_3$. On K_2NiF_4 -type $La_{0.2}Sr_{1.8}MnO_4$, on the other hand, XRD result suggested the formation of not PdO but $SrPd_3O_4$. Fig. 3 shows TPD chromatograms of oxygen from Pd/ $La_{0.2}Sr_{1.8}MnO_4$ and Pd/ $La_{0.5}Sr_{0.5}MnO_3$. Oxygen desorption corresponding the decomposition of PdO to Pd metal was observed for Pd/ $La_{0.5}Sr_{0.5}MnO_3$, confirming the presence of PdO on the perovskite support. On the other hand, no oxygen desorption was observed for Pd/ $La_{0.2}Sr_{1.8}MnO_4$. This indicates that the stability of Pd^{2+} ion against the thermal reduction (decomposition) is enhanced by the formation of a mixed metal oxide, $SrPd_3O_4$ in this case.

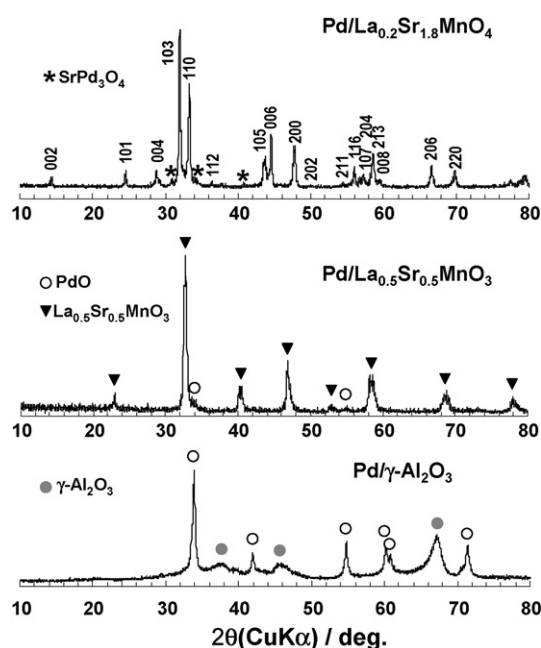


Fig. 2. XRD patterns of Pd/ $La_{0.2}Sr_{1.8}MnO_4$, Pd/ $La_{0.5}Sr_{0.5}MnO_3$, Pd/ $\gamma-Al_2O_3$.

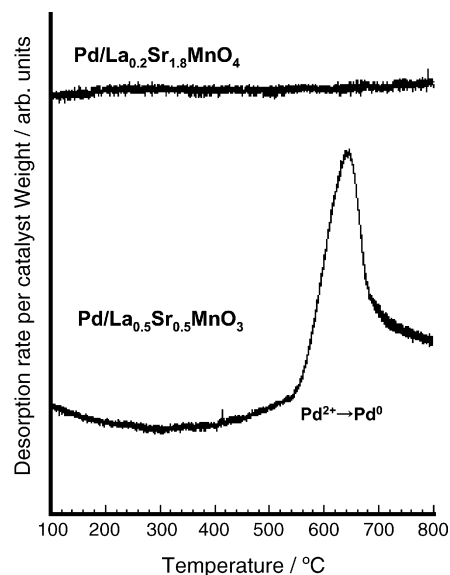


Fig. 3. TPD chromatograms of oxygen from Pd/ $La_{0.2}Sr_{1.8}MnO_4$ and Pd/ $La_{0.5}Sr_{0.5}MnO_3$.

When $La_{0.2}Sr_{1.8}MnO_4$ was suspended in water, the dissolution of only Sr^{2+} was observed; the amount of Sr^{2+} dissolved after 20 h was about 7% of total Sr^{2+} originally present in the oxide. The fundamental K_2NiF_4 -type crystal structure was preserved after the dissolution of Sr^{2+} , probably indicating the formation of an A-site deficient oxide. It seems that the dissolved Sr ions are deposited on Sr-deficient $La_{0.2}Sr_{1.8-8}MnO_4$ together with Pd ions during the evaporation-to-dryness process and that deposited Sr and Pd ions are react to form $SrPd_3O_4$ in the air-calcination step. The Sr dissolution and $SrPd_3O_4$ formation were also observed for $La_{0.4}Sr_{1.6}MnO_4$.

3.2. Catalytic property

The temperature dependences of the NO–CO reaction over $La_xSr_{2-x}MnO_4$ ($0 \leq x \leq 0.8$) are shown in Fig. 4(A). Judged from the CO conversion to CO_2 , the activity of Sr_2MnO_4 was quite lower than the others, indicating the advantage of forming the K_2NiF_4 -type structure. With increasing the La content (x), the activity first increased up to $x = 0.5$ and then decreased at $x = 0.6$ and 0.8. Since the solubility limit of La was around $x = 0.5$, it can be said that the catalytic activity of $La_xSr_{2-x}MnO_4$ increases with increasing the La content within the composition range to form the single-phase K_2NiF_4 -type oxide. The decrease in activity at $x = 0.6$ and 0.8 must be caused by the presence of La_2O_3 ; the catalytic activity of another by-product of $SrMnO_{3-8}$ was comparable to or even higher than that of $La_{0.5}Sr_{1.5}MnO_4$ (see below). It seems that the amount of La_2O_3 in the oxide with $x = 0.5$ is too small to interfere the high activity of the main K_2NiF_4 -type oxide. The catalytic activity of perovskite-related oxides is often discussed in relation to the oxidation state of transition metal ions and the oxygen nonstoichiometry. As can be seen from Table 1, clear dependence on the oxide composition was observed not for

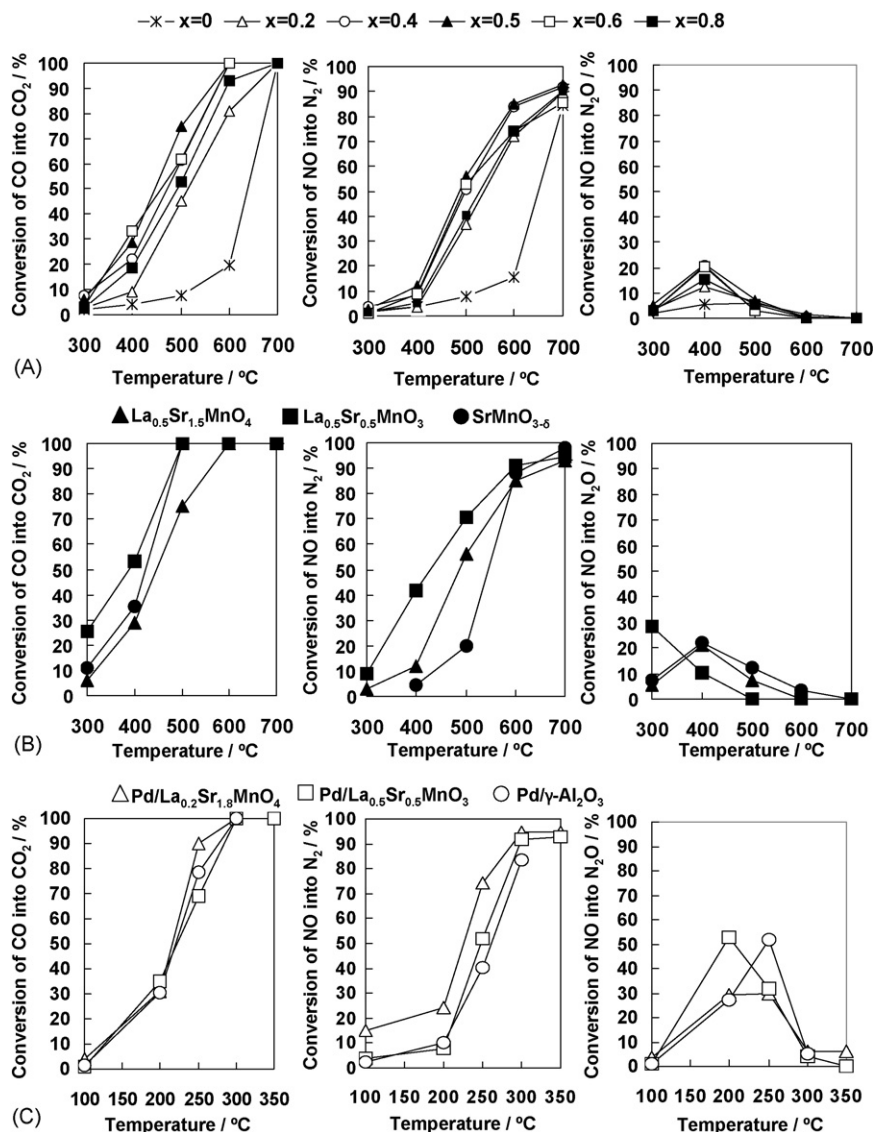


Fig. 4. Catalytic activity for NO–CO reaction. (A) $\text{La}_x\text{Sr}_{2-x}\text{MnO}_4$ ($0 \leq x \leq 0.8$), (B) $\text{La}_{0.5}\text{Sr}_{1.5}\text{MnO}_4$, $\text{La}_{0.5}\text{Sr}_{0.5}\text{MnO}_3$ and $\text{SrMnO}_{3-\delta}$, (C) $\text{Pd/La}_{0.2}\text{Sr}_{1.8}\text{MnO}_4$, $\text{Pd/La}_{0.5}\text{Sr}_{0.5}\text{MnO}_3$, $\text{Pd}/\gamma\text{-Al}_2\text{O}_3$.

the oxidation state of Mn ion but for the oxygen nonstoichiometry. It might be said that the catalytic activity of $\text{La}_x\text{Sr}_{2-x}\text{MnO}_4$ is low and high for the oxygen-deficient and oxygen-excess oxides, respectively.

As shown in Fig. 4(B), the catalytic performance of $\text{La}_{0.5}\text{Sr}_{1.5}\text{MnO}_4$, which was the most active in $\text{La}_x\text{Sr}_{2-x}\text{MnO}_4$ ($0 \leq x \leq 0.8$), was inferior to that of $\text{La}_{0.5}\text{Sr}_{0.5}\text{MnO}_3$. $\text{La}_{0.5}\text{Sr}_{1.5}\text{MnO}_4$ was inferior and superior to $\text{SrMnO}_{3-\delta}$ in terms of activity (CO conversion) and selectivity to N_2 formation, respectively. When used as the support for Pd, however, $\text{La}_x\text{Sr}_{2-x}\text{MnO}_4$ gave an excellent catalyst system (Fig. 4(C) for $x = 0.2$). The Pd-loaded catalysts showed higher activity than the corresponding Pd-free catalyst, for example, $\text{Pd/La}_{0.2}\text{Sr}_{1.8}\text{MnO}_4$ versus $\text{La}_{0.2}\text{Sr}_{1.8}\text{MnO}_4$, clearly indicating that Pd serves as an active species in the Pd-loaded catalysts. As can be seen from Fig. 4(C), $\text{Pd/La}_{0.2}\text{Sr}_{1.8}\text{MnO}_4$ showed

comparable to or even higher activity than $\text{Pd/La}_{0.5}\text{Sr}_{0.5}\text{MnO}_3$ and $\text{Pd}/\gamma\text{-Al}_2\text{O}_3$. In addition, $\text{Pd/La}_{0.2}\text{Sr}_{1.8}\text{MnO}_4$ was more selective to N_2 formation than the other two catalysts; N_2 selectivity at 250 °C was 71.4% ($\text{Pd/La}_{0.2}\text{Sr}_{1.8}\text{MnO}_4$), 62.0% ($\text{Pd/La}_{0.5}\text{Sr}_{0.5}\text{MnO}_3$) and 43.6% ($\text{Pd}/\gamma\text{-Al}_2\text{O}_3$). Taking the characterization results into accounts, it can be said that the excellent catalytic performance of $\text{Pd/La}_{0.2}\text{Sr}_{1.8}\text{MnO}_4$ as compared with $\text{Pd/La}_{0.5}\text{Sr}_{0.5}\text{MnO}_3$ and $\text{Pd}/\gamma\text{-Al}_2\text{O}_3$ can be ascribable to the presence of SrPd_3O_4 . XPS investigation showed that BE values of $\text{Pd}3d_{5/2}$ were almost the same for $\text{Pd/La}_{0.2}\text{Sr}_{1.8}\text{MnO}_4$ (336.3 eV) and $\text{Pd/La}_{0.5}\text{Sr}_{0.5}\text{MnO}_3$ (336.4 eV). This indicates that the electronic state of Pd^{2+} was the same between SrPd_3O_4 on $\text{La}_{0.2}\text{Sr}_{1.8}\text{MnO}_4$ and PdO on $\text{La}_{0.5}\text{Sr}_{0.5}\text{MnO}_3$. The catalytic property of SrPd_3O_4 should be clarified in a future study. It is noted that the catalytic property of alkaline earth-Pd mixed metal oxides was not so far reported

though that of rare earth (Ln)–Pd mixed metal oxides, Ln_4PdO_7 , was reported [17–19].

4. Conclusions

Mn-based K_2NiF_4 -type oxides, $\text{La}_x\text{Sr}_{2-x}\text{MnO}_4$, were found to be obtained as single-phase oxides in the range of $0.1 \leq x < 0.5$ under the preparation condition of air-calcination at 800 °C, which is easily used in the catalytic investigation. Catalytic activity of $\text{La}_x\text{Sr}_{2-x}\text{MnO}_4$ for NO–CO reaction increased with increasing x in the range of solubility limit of La, and $\text{La}_{0.5}\text{Sr}_{1.5}\text{MnO}_4$ showed the highest activity. The catalytic activity of $\text{La}_x\text{Sr}_{2-x}\text{MnO}_4$ was inferior to that of perovskite-type $\text{La}_{0.5}\text{Sr}_{0.5}\text{MnO}_3$, but $\text{La}_x\text{Sr}_{2-x}\text{MnO}_4$ gave the excellent catalytic system with high activity and selectivity to N_2 when used as the support for Pd loading. The formation of SrPd_3O_4 in Pd/ $\text{La}_x\text{Sr}_{2-x}\text{MnO}_4$ might be a reason for the excellent catalytic property of Pd/ $\text{La}_x\text{Sr}_{2-x}\text{MnO}_4$. Although the catalytic nature of SrPd_3O_4 should be clarified, the present study strongly suggests the potentiality of mixed metal oxides of noble metals, SrPd_3O_4 in the present case, as active species in three-way catalysis. In addition, the formation of SrPd_3O_4 was realized in this study by the dissolution of Sr^{2+} from the support and its re-deposition with Pd^{2+} . The dissolution/re-deposition phenomena might be used as a new method to prepare supported catalysts of mixed metal oxides of noble metals.

References

- [1] L.J. Tejuca, J.L.G. Fierro, Properties and Applications of Perovskite-type Oxides, Marcel Dekker, Inc., New York, 1993.
- [2] H. Tanaka, I. Tan, M. Uenishi, M. Kimura, K. Dohmae, Top. Catal. 16/17 (2001) 63–70.
- [3] Y. Nishihata, J. Mizuki, T. Akao, H. Tanaka, M. Uenishi, M. Kimura, T. Okamoto, N. Hamada, Nature 418 (2002) 164–167.
- [4] K.V. Ramanujachary, N. Kameswari, C.S. Swamy, J. Catal. 86 (1984) 121.
- [5] T. Nitadori, M. Misono, Chem. Lett. 1255 (1986).
- [6] T. Nitadori, M. Muramatsu, M. Misono, Bull. Chem. Soc., Jpn. 61 (1988) 3831.
- [7] T. Nitadori, S. Kurihara, M. Misono, Chem. Mater. 1 (1989) 215.
- [8] A.K. Ladavos, P.J. Pomonis, J. Chem. Soc., Faraday Trans. 87 (1991) 3291.
- [9] S. Rajadurai, J.J. Carberry, B. Li, C.B. Alcock, J. Catal. 131 (1991) 582.
- [10] A.K. Ladavos, P.J. Pomonis, J. Chem. Soc., Faraday Trans. 88 (1992) 2557.
- [11] A.K. Ladavos, P.J. Pomonis, Appl. Catal. B 1 (1992) 101.
- [12] H. Yasuda, T. Nitadori, N. Nizuno, M. Misono, Bull. Chem. Soc., Jpn. 66 (1993) 3494.
- [13] Y. Wu, Z. Zhao, Y. Liu, X. Yang, J. Mol. Catal. A 155 (2000) 89.
- [14] X. Yang, L. Luo, H. Zhong, Appl. Catal. A 272 (2004) 299.
- [15] M. Karppinen, M. Matvejeff, K. Salomäki, H. Yamauchi, J. Mater. Chem. 12 (2002) 1761.
- [16] N. Mizutani, A. Kitazawa, N. Okuma, M. Kato, Kogyo Kagaku Zasshi 73 (1970) 1097.
- [17] M. Andersson, K. Jansson, M. Nygren, Catal. Lett. 39 (1996) 253.
- [18] M. Andersson, K. Jansson, M. Nygren, Thermochim. Acta 318 (1998) 83.
- [19] M. Andersson, E. Bakchinova, K. Jansson, M. Nygren, J. Mater. Chem. 9 (1999) 265.